A Computational and Conceptual DFT Study on the Michaelis Complex of pI258 Arsenate Reductase. Structural Aspects and Activation of the Electrophile and Nucleophile

Goedele Roos,[†,§] Joris Messens,[‡] Stefan Loverix,[†,‡] Lode Wyns,[‡] and Paul Geerlings*[,†]

Algemene Chemie (ALGC), Vrije Universiteit Brussel (VUB), Pleinlaan 2, B-1050, Brussels, Belgium, and Departement Ultrastructuur, Vlaams interuniversitair Instituut voor Biotechnologie (VIB), Vrije Universiteit Brussel (VUB), Pleinlaan 2, B-1050, Brussels, Belgium

Received: March 26, 2004; In Final Form: June 24, 2004

The first step in the reduction of arsenate to arsenite catalyzed by the enzyme arsenate reductase (ArsC) from *Staphylococcus aureus* plasmid pI258 involves the nucleophilic attack of a cysteine thiolate (Cys10) on the arsenic atom, leading to a covalent sulfur−arseno intermediate. We present a quantum chemical study on the onset of the nucleophilic displacement reaction. To optimize the reactant state geometry, a density functional study was performed on Cys10, on dianionic arsenate, and on the catalytic site sequence motif: X-X-Asn13-X-X-Arg16-Ser17. Both the hydrogen bond from Arg16 to the leaving hydroxyl group of arsenate and the hydrogen bonds from various backbone amide nitrogens of the catalytic site to the other oxygen atoms of arsenate are responsible for the increased electrophilicity of the central arsenic atom. In particular, Arg16 is identified as a residue that destabilizes the groundstate of the complex. Furthermore, the binding of dianionic arsenate to the enzyme induces negative charge transfer from the substrate to ArsC, which renders arsenic more receptive to nucleophilic attack. On the other hand, an α-helical macrodipole and a K^+−Cys10 interaction network via Asn13 and Ser17 activate the nucleophile and stabilize the thiolate form of Cys10 by lowering its pK_a to 6.7. By dissection of these interactions and performance of a reactivity analysis, the experimentally measured steady-state kinetic data and the function of crucial interactions observed in the X-ray structures of ArsC are illuminated.

Introduction

Arsenate reductase (ArsC) (Figure 1A), the *arsC* gene product from *Staphylococcus aureus* pI258 plasmid, has a low molecular weight phosphatase (LMW PTPase) anion-binding motif[1]—known as the P-loop. It is composed of a nucleophilic cysteine (Cys10), an asparagine (Asn13), an arginine (Arg16), and a serine (Ser17): Cys10-XX-Asn13-XX-Arg16-Ser17 (ArsC numbering),[1] which forms the catalytic site in both ArsC[1] and LMW PTPase.[2] The amino acid sequence of the ligand-binding loop in pI258 ArsC is:[1] Cys10-Thr11-Gly12-Asn13-Ser14-Cys15-Arg16-Ser17. The first step of the catalytic mechanism of ArsC consists of a phosphatase-like nucleophilic displacement reaction carried out by Cys10 on arsenate[1] (Figure 1B). In the case of PTPases, there is a disagreement regarding the exact reaction mechanism. In a first interpretation, the catalytic cysteine in the form of a thiolate attacks the substrate in its dianionic form.[2,3] An alternative theory argues against the three negative charges in the Michaelis complex and proposes that the substrate binds as a monoanion.[4] A variant of this mechanism considers the existence of the cysteine in the thiol form, suggesting the dianionic substrate accepts a proton to activate the nucleophilic thiol to a thiolate.[4] Until today, no mechanistic studies have been performed on ArsC. However, in a HSAB[6] context, it is seen from our preceding work[5] that the reactivity described by the local softness of a thiolate toward dianionic arsenate is higher than toward other protonation states of arsenate. So a reaction mechanism in which the nucleophilic attack is done by a −1 charged thiolate on a −2 charged substrate has been suggested—a counterintuitive idea that will be documented.

The pH optimum for enzymatic catalysis by ArsC enzymes from various species lies in the range 6.3−8.0.[7] In this pH range, free cysteine (pK_a = 8.3) is largely present in the thiol form which is a far inferior nucleophile than the thiolate form.[8] However, the acid/base properties of functional groups may be perturbed in a protein environment as compared to aqueous solution.[9]

In pI258 ArsC, a hydrogen bond network[10] involving S_γCys10, Ser17, and Asn13, terminated by the electrostatic interaction with a potassium ion (called the C10−K^+ interaction network, further on) (Figure 2), is observed in all the X-ray structures of pI258 ArsC present in the PDB.[1,11] ArsC also possesses an α-helix (extending from amino acid 16 to 29)[1] of which the N-terminal side faces the nucleophile. The experimental determination of the pK_a of the Cys10 thiol group is not straightforward because three redox active intramolecular cysteine residues are involved in the successive steps of the reaction mechanism[1] (Figure 1B). On the basis of high level quantum chemical calculations, the effect of the C10−K^+ interaction network and the macrodipole arising from the α-helix on the pK_a of the Cys10 functional group will be revealed.

All essential intermediates in the reaction mechanism of ArsC have been visualized with X-ray crystallography supplemented by NMR,[11] with the exception of a Michaelis complex. We will focus on the onset of the nucleophilic displacement reaction by Cys10 in ArsC and we will present a theoretically optimized ArsC-arsenate complex with a concomitant in-depth description of the enzyme−substrate interactions, using both computational[12] and conceptual[13] density functional theory (DFT).

* Corresponding author. Telephone: +32 2629 33 14. Fax: +32 2629 33 17. E-mail: pgeerlin@vub.ac.be.

† Algemene Chemie (ALGC), Vrije Universiteit Brussel (VUB).

‡ Departement Ultrastructuur, Vlaams interuniversitair Instituut voor Biotechnologie (VIB), Vrije Universiteit Brussel (VUB).

§ E-mail: Goedele Roos: groos@vub.ac.be.

10.1021/jp0486550 CCC: $27.50
Published on Web 10/14/2004

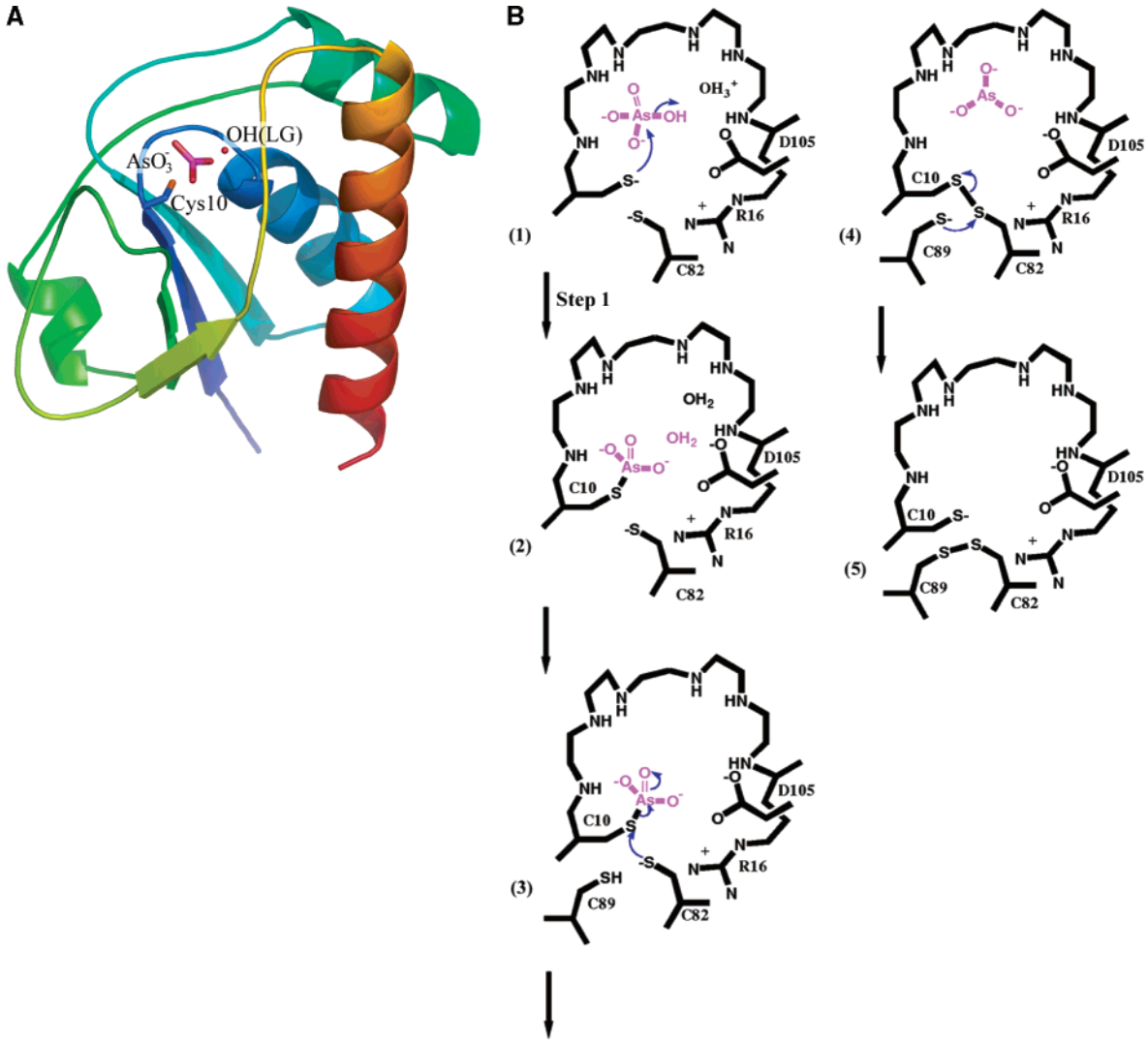

Figure 1. (A) Ribbon diagram of the overall structure of the arsenic bound intermediate of pI258 ArsC (PDB: 1LJU). The nucleophilic Cys10 and the leaving hydroxyl are shown. (B) Scheme of the reaction mechanism of pI258 ArsC.[11] The reaction starts (1) with the nucleophilic attack of Cys10 on arsenate leading to a covalent intermediate (2). Arsenite is released after the nucleophilic attack of the thiol of Cys82. The electrons of the S−As bond shuttle to arsenic (3). A Cys10-Cys82 intermediate is formed (4). Finally, Cys89 attacks Cys82, forming a Cys82-Cys89 disulfide on the surface of the redox enzyme (5).

Dissecting these interactions and performing a reactivity analysis provide insight into the structural features of ArsC related to its capability to activate both the electrophile (arsenate) and the nucleophile (Cys10) in the reactant state. The experimentally measured steady-state kinetic data are elucidated and crucial interactions in the X-ray structures of ArsC are explained by looking to the properties of some critical residues into the ground state.

Enzymatic catalysis already starts with the binding of the substrate. Therefore, we carefully studied the ground state of this redox enzyme. The theoretically obtained results presented here give us the ability to draw conclusions that were inaccessible only based on the X-ray and steady-state kinetic data. As such, within the framework of ongoing studies[14] combining theoretical and experimental investigations, our theoretical work gives an extra dimension in the elucidation of the catalytic mechanism of ArsC.

Theory and Computations

DFT Description of Reactivity. The hard and soft acids and bases principle (HSAB) has been shown to be useful to describe both kinetic and thermodynamic aspects of a chemical reaction (onset of the reaction, relative stability of reactants and products). This principle formulated by Pearson[6] states that hard bases prefer hard acids and soft bases, soft acids. The physical underpinning of the HSAB principle is founded in density functional theory[12] and is, together with other principles and reactivity descriptors, part of conceptual density functional theory.[13] Thiolates and arsenate are soft (polarizable) species. As a consequence a soft−soft mechanism underlies the reactivity of ArsC, which at the local level (cf. ref 15a) can be quantified by the difference in local softness $s(\mathbf{r})$ of the interacting parts, the sulfur and arsenic atoms of the respective reactants Cys10 and arsenate.

$$\Delta s(\mathbf{r}) = |s^{+}(\mathbf{r}) - s^{-}(\mathbf{r})| \quad (1)$$

This difference should be minimal for optimal interaction.

The local softness $s(r)$ is obtained as

$$s(\mathbf{r}) = f(\mathbf{r})S \quad (2)$$

where S is the global softness of the system[15a] and $f(\mathbf{r})$ the Fukui function,[15b] a frontier MO reactivity index. $f(\mathbf{r})$ measures the

electron density $\rho(\mathbf{r})$ response upon electron donation to the system (nucleophilic attack) $f^+(\mathbf{r})$, or electron withdrawing (electrophilic attack) $f^-(\mathbf{r})$. Using electron population analysis, $f(\mathbf{r})$ can be condensed to atoms, providing atom-centered reactivity indices f_A:

$$f_A^- = q_A(N_0) - q_A(N_0 - 1) \quad (3)$$

$$f_A^+ = q_A(N_0 + 1) - q_A(N_0) \quad (4)$$

$q_A(N_0)$, $q_A(N_0+1)$, and $q_A(N_0 - 1)$ are the atomic populations for atom A in the neutral molecule (N_0 electrons) and the corresponding anion ($N_0 + 1$) or cation ($N_0 - 1$), all evaluated at the neutral (as reference) molecular geometry, as requierd by the constant external (i.e. due to the nuclei) potential $\nu(\mathbf{r})$ in the definition of the Fukui function.

As a direct consequence of eqs 3 and 4, two types of local (condensed) softness are defined:

$$s_A^- = Sf_A^- \quad (5)$$

$$s_A^+ = Sf_A^+ \quad (6)$$

In our study s^+ indicates the local softness of arsenic and s^- the local softness of sulfur.

Using a finite difference approximation together with Koopman's theorem,[16] the global softness S can be approximated by

$$S = 1/(\epsilon_{LUMO} - \epsilon_{HOMO}) \quad (7)$$

with ϵ_{HOMO} the energy of the highest occupied molecular orbital and ϵ_{LUMO} the energy of the lowest unoccupied molecular orbital. In our previous study,[5] eq 7 was proven to be a good approximation for S, even in a DFT context.

A quantitative measure of the electrophilicity of a species provides another useful tool for the rationalization of chemical reactivity. Starting from the question to what extent electron-transfer contributes to the lowering of the total binding energy by maximal flow of electrons, Parr et al.[17a] provide validation for the qualitative suggestion made by Maynard and co-workers[17b] for the electrophilic power of a ligand.

On the basis of a second-order model for the change in the electronic energy as a function of the changes in the number of electrons ΔN, at constant external potential $\nu(\mathbf{r})$, namely

$$\Delta E = \mu\Delta N + \eta\Delta N^2/2 \quad (8)$$

with μ the electronic chemical potential and η the chemical hardness; the electrophilicity index ω may be obtained from minimizing ΔE with respect to ΔN. The result can be written as

$$\omega = \mu^2/\eta \quad (9)$$

or in a finite difference approximation

$$\omega = (I + A)^2/8(I - A) \quad (10)$$

where I and A are the ionization energy and the electron affinity respectively, calculated as the difference in total energies between the neutral and the corresponding ionic species. The multiplication of eq 9 by the condensed Fukui function f_A^+ yields a regional electrophilicity index[17c] ω^+ for atom A.

$$\omega^+ = \omega f_A^+ \quad (11)$$

For recent extensions to the spin polarized case, see ref 18.

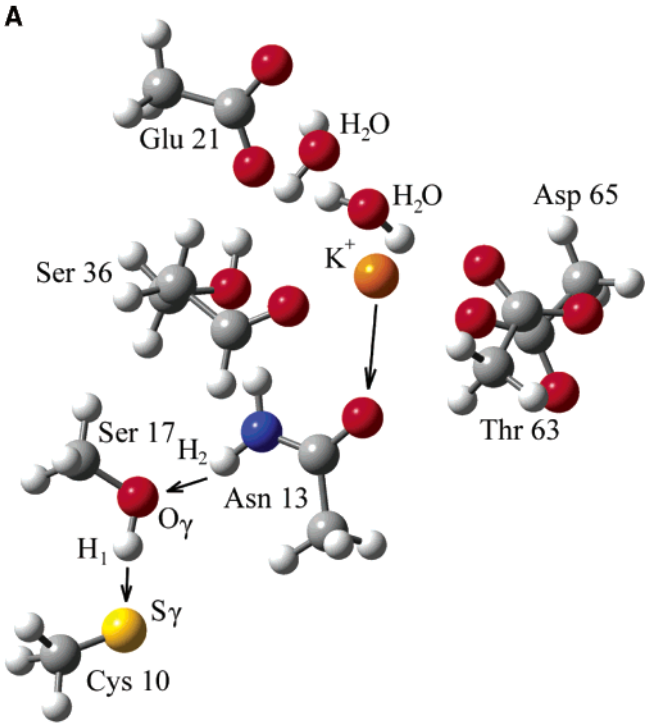

B

	H_2--O_γ	H_1--S_γ	*Cys10--Ser17* HBS *(kcal/mol)*
WT`	1.960	1.690	**-6.90**
Asn13 - mutant	/	1.700	-6.30
K+ - mutant	1.968	1.700	-6.33
Asn13 -/K+ - mutant	/	1.710	**-5.68**

Figure 2. (A) WT′ model. The Asn13, K^+, and the double mutant are constructed from this model. In all of the model systems, the hydrogen atoms were optimized at the B3LYP/6-31+G* level. The coordinates of the heavy atoms are taken from the PDB structure 1JF8[1] (see Model Systems and Computational Details, section Activation of the Nucleophile). Color code: hydrogen, white; nitrogen, blue; carbon, gray; sulfur, yellow; potassium, orange. (B) Hydrogen bond distances (Å) in the S_γCys10, Ser17, Asn13, potassium network. Cys10-Ser17 hydrogen bond strength (HBS) (kcal/mol) calculated at the B3LYP/6-31+G** level.

Model Systems and Computational Details. *Optimization of the Michaelis Complex.* pI258 ArsC is a relatively small enzyme (131 amino acids),[1] but there are still too many electrons for high level quantum calculations. Therefore, the enzyme needs to be described by an adequate model, combining accuracy with computational tractability. The model system of choice was constructed starting from the X-ray structure (resolution 1.4 Å) of the Cys15Ala mutant of ArsC complexed with arsenite (product of the first reaction step, PDB 1LJU).[11] Our model included the complete conserved catalytic sequence motif, Cys10-X-X-Asn13-X-X-Arg16-Ser17, since the backbone amides of this substrate binding loop form hydrogen bonds with the oxygen atoms of the substrate. Amino acids 10 and 17 were terminated respectively with $-NH_2$ and $-CONH_2$. The side chains of residues 11, 12, 14, and 15 were terminated on a C_α, since they are positioned at the periphery of the substrate binding loop where no interaction with the substrate occurs. The three well positioned water molecules present in the active site of the PDB structure 1LJU were incorporated. Dianionic arsenate was taken as substrate. Since the hydrogen atom positions cannot

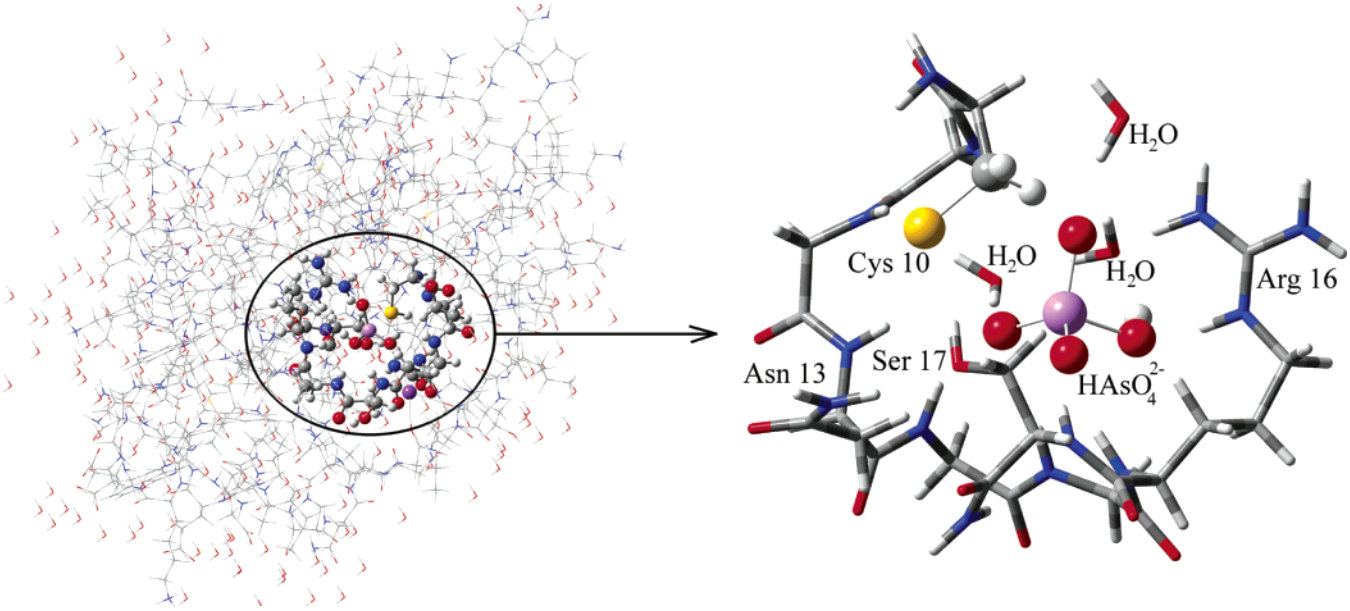

Figure 3. Reduction of the X-ray structure of ArsC (PDB: 1LJU)[11] to the WT model (See text for details). Partitioning of the WT model system of ArsC into two layers: high level represented in "Ball & Stick"; low level in "Tube". A similar division is made for the Asn13Ala and the Arg16Ala mutants. Color code: hydrogen, white; nitrogen, blue; carbon, gray; oxygen, red; sulfur, yellow; arsenic, purple.

be discerned from a 1.4 Å resolution X-ray structure, they were placed with the SPARTAN[19a] package and subsequently minimized by means of the Merck force field (MMFF).[19b] The resulting model is called "wild type (WT)" throughout (Figure 3). The Arg16Ala and the Asn13Ala mutants were built "in silico",[14b−d] starting from the coordinates of the WT model.

The geometry of the structures of the WT and the Asn13Ala and the Arg16Ala mutants were optimized using a QM/QM ONIOM[20−23] multilayer model. The ONIOM method has been proven to be a powerful tool for the theoretical treatment of the structure of large molecular systems.[22] The strength of this method lies in the fact that highly accurate calculations on large systems are made possible by partitioning the systems into different layers (in general two or three), each of them treated at a different level of theory. By this approach, electron correlation effects can be included in quantum calculations of large systems (i.e. more than 100 atoms). The wild type, Asn13Ala, and Arg16Ala model systems of ArsC were partitioned into two layers (Figure 3). The most relevant parts, being the nucleophile and the substrate, form the inner layer and were treated at a "high" level of theory, namely at the DFT level, using the Becke three-parameter Lee Yang−Parr (B3LYP) exchange correlation potential, through which electron correlation effects are included, with a 6-31+G** basis set. The remaining part of the system, the ligand binding loop, constituted the outer layer and was described by a computationally less demanding method, Hartree−Fock with a 6-31G basis set.

Interactions with the Electrophile. Gas-phase free arsenate was used as the reference state in the study of the enzyme bound ligand. The structure of this arsenate molecule has been optimized at the B3LYP/6-31+G** level.

For comparison of the charge distribution between enzyme bound and free arsenate in the gas phase, the NPA population analysis,[24] calculated at the B3LYP/6-31+G** level, is used. This choice is founded on the many successful applications of this population analysis in the study of molecular properties.[25] In contrast, Mulliken charges are not advisable to use because of their strong basis set dependence,[26] whereas electrostatic potential derived charges (e.g., ChelpG) are not recommended in view of the ChelpG charge-deriving scheme[27] from which one can suspect a poor description of ligands embedded in large systems,[28] our point of interest.

Interactions with the Nucleophile. To study the effect of the C10−K^+ interaction network on the nucleophilic Cys10, a model system was dissected from the X-ray structure of ArsC Cys10Ser/Cys15Ala (PDB 1JF8).[1] This model included Cys10, Ser17, Asn13, potassium, and the potassium binding pocket[10] consisting of Asp65, Glu21 Thr63, Ser36 Asn13, and two water molecules. On the basis of the hydrogen bond interactions present and the interactions with the potassium ion, Cys10 is modeled as CH_3S^-, Ser17 as CH_3OH, Asn13 as $NH_2-CO-CH_3$, Glu21, Thr63 (backbone), and Asp65 as CH_3-COO^-, and Ser36 as $HOCH_2-CH_2-COH$. This model is called WT′ (Figure 2). Starting from the WT′ model, the Ser17 mutant, the Asn13 mutant (−Asn13), the potassium mutant (−K^+), and the double mutant (−Asn13/- K^+) were created.

Mutation of the Asn13 side chain might prevent binding of the potassium ion, leading to structural perturbations in the protein. A theoretical study offers the opportunity to dissect the C10−K^+ interaction network and thus to study the role and impact of every single residue in the activation of Cys10. In the considered models, the hydrogen atoms were placed manually with MMFF[19b] implemented in the SPARTAN[19a] package and then optimized at the B3LYP/6-31+G* level, while the coordinates of the heavy atoms (carbon, nitrogen and oxygen) were taken from the X-ray structure (PDB: 1JF8).

To calculate the hydrogen bond strength between Cys10 and Ser17, after the optimization of the hydrogen atoms, the model was simplified to a two-component system consisting of Cys10 and Ser17. The error caused by the basis set superposition, the basis set superposition error (BSSE), was taken into account by the counterpoise correction (CP) proposed by Boys and Bernardi.[29]

Since DFT provides reliable hydrogen bond strengths,[12b,14b,30] our calculations were performed in a DFT context, at the B3LYP/6-31+G** level.

When studying the effect of the α-helix (extending from amino acid 16 to 29), the dipole of the helix was taken into

A

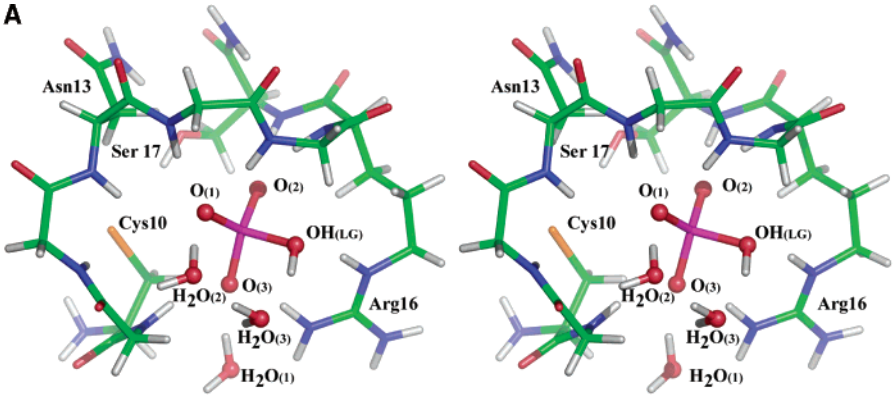

B

Donor--Acceptor	*l(Å)*	*a(°)*
$N_{\varepsilon}H$(Arg16)--OH(LG)	2.82	168
OH(LG)--OH_2(1)	2.70	147
$N_{16}H$--O(1)	2.86	153
$N_{17}H$--O(1)	2.79	166
HOH(2)--O(2)	2.69	170
$N_{14}H$--O(2)	2.83	153
$N_{11}H$--O(3)	2.84	150
$N_{\eta}H$(Arg16)--O(3)	2.74	164
HOH(3)--O(3)	2.70	167

Figure 4. (A) Stereoview of the optimized (two-layer ONIOM scheme: B3LYP/6-31+G**//HF/6-31G) Michaelis complex. (B) Enzyme−substrate interactions in the Michaelis complex. HOH(*x*)- -O(*y*) points to a hydrogen bond between HOH number *x* as proton donor and the substrate oxygen atom number *y* as proton acceptor. *l* gives the distance between donor and acceptor in Å and *a* gives the angle between donor-proton-acceptor in deg. LG stands for leaving group and N_xH for the backbone amide group of the amino acid with number *x*.

account by representing the atoms of the helix as point charges. Before calculating these charges, the hydrogen atoms were placed by minimization with MMFF[19b] implemented in the SPARTAN package.[19a] No quantum chemical optimization was carried out after this step. Since the point charges are required to describe the electrostatic effects of the helix, the electrostatic potential derived ChelpG[27] population analysis executed at the B3LYP/6-31G** level was chosen.[31] One should remark that the 14 amino acids of the helix form a too large system to perform a ChelpG population analysis, so that a reduction of the helix to a model is required. To verify the notion that mainly the backbone of the helix contributes to the macrodipole, we compared the effect of the Mulliken charges of the α-helix on the proton affinity of Cys10 with the effect of the Mulliken charges of a so-called "Ala-helix" (obtained by terminating every amino acid different from Gly at C_{β}). This comparison gives only a negligible difference of 1 kcal/mol on a proton affinity of 400 kcal/mol, permitting us to use the "Ala-helix" safely to study the effect of the dipole of the α-helix on Cys10.

To explore and quantify the effect of the C10−K^+ interaction network and the α-helix on the basicity of Cys10, we calculated the proton affinity of Cys10 in the presence and absence of the components of the C10−K^+ interaction network and the α-helix. Proton affinities were calculated at the B3LYP/6-31+G** level by subtracting the energies of the optimized (B3LYP/6-31+G*) protonated and deprotonated forms. To translate changes in proton affinity to changes in the acid dissociation constant (pK_a), we calculated proton affinities of a series of five thiolates (methanethiol, benzenemethanethiol, mercaptoethanol, cysteine, and trifluoroethanethiol) and plotted these values against experimental pK_a values (Figure 5). The resulting linear relationship was used to extrapolate the pK_a of Cys10 in the considered models from its calculated proton affinity. Ideally, for this purpose, aqueous proton affinities[32] should be used. However, gas-phase proton affinities gave a superior correlation to the one obtained in water, using the advanced SCI−PCM[33] model. This might be due to the absence of the hydrogen bond interactions between the thiol/thiolate group of the solute and the surrounding solvent when using the continuum model.

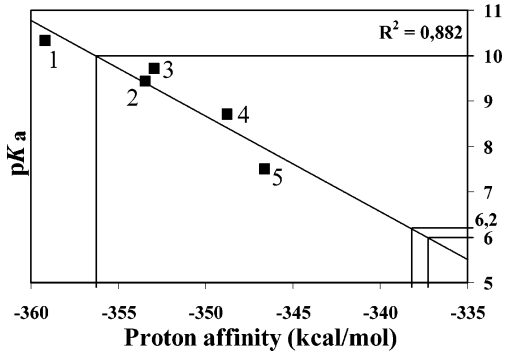

Figure 5. Proton affinity−pK_a correlation curve calculated in the gas phase for a series of five substituted thiolates: 1 = methanethiol; 2 = benzenemethanethiol; 3 = mercaptoethanol; 4 = cysteine; 5 = trifluoroethanethiol. The effect of the hydrogen bond network on the pK_a of Cys10 is shown. The calculated proton affinities of Cys10 in the presence of different elements of the C10−K^+ interaction network are inserted. 10.0: pK_a of Cys10 in the presence of a solitary SγCys10-H−OγSer17 hydrogen bond. 6.2: pK_a of Cys10 in the presence of the C10−K^+ interaction network. 6.0: pK_a of Cys10 in the presence of the C10−K^+ interaction network + α-helix dipole effect

DFT Measures of Reactivity. An electrostatic model was used as an approximation for the influence of ArsC on the reactivity indices of arsenate and CH_3S^- (as model for Cys10). Arsenate was embedded in the enzymatic environment of the WT and Arg16Ala model systems, while the environments of WT′ and $-$Asn13/$-K^+$ were used to surround CH_3S^-. The enzymatic environment of wild type and mutant ArsC was represented by ChelpG point charges, calculated at the B3LYP/6-31G** level.[27,31]

NPA charges[24,25] calculated at B3LYP/6-31+G** were used to obtain the Fukui function.

All calculations were performed using the GAUSSIAN 03 package.[34]

Results and Discussion

Theoretically Optimized Michaelis Complex. *Calculated Model.* Starting from the X-ray structure of ArsC complexed with arsenite, i.e., the product of the first reaction step (PDB: 1LJU)[11] (Figure 1), a model of the enzyme−substrate (Michaelis) complex of ArsC is optimized using a two-layer QM/QM ONIOM[21−24] scheme (B3LYP/6-31+G**//HF/6-31G) (Figure 3). To check whether this structure is an acceptable Michaelis complex, the same methodology used to obtain the ArsC Michaelis complex was also applied to a productlike structure of a protein tyrosine phosphatase (PTPase) of the *Yersinia* bacteria in complex with NO_3^- (PDB: 1YTN),[35] which is analogous to AsO_3^-. This calculated PTPase Michaelis complex was compared with the experimental X-ray structure of a complex with a tetrahedral oxyanion (Michaelis complex-like structure) of the same *Yersinia* PTPase (PDB: 1YTS).[36] All the observed enzyme−substrate interactions in 1YTS were retrieved in the optimized Michaelis complex. In analogy with this result, the structure of the ArsC Michaelis complex obtained from 1LJU by using the QM/QM ONIOM scheme (B3LYP/6-31+G**//HF/6-31G) can be treated with confidence.

The dihedral angles of the peptide bonds found in the optimized enzyme−substrate complex of ArsC deviate on average by 7° from planarity (between a deviation maximum and minimum of 11 and 2°, respectively). Experimental statistical data report deviations from the exact planar peptide bond up to 6°[36] and even more when circular peptides are considered.[37] As such, in the ligand binding pocket of ArsC, which has a circular geometry, the averaged deviation from peptide bound planarity can be considered as acceptable and the activation barriers of peptide bond rotations are properly described by the proposed ONIOM scheme.

Structure Stabilization. One of the mechanisms used by enzymes to reduce the activation barrier is the constitution of an environment that prepares the substrate(s) to undergo the reaction to product(s), as formulated in the "environmental preorganization concept".[38a,b] This concept has long been seen as a special feature of enzymes, but is nowadays largely questioned (for an extended discussion, see ref 38). In the case of ArsC, the empty active site is not structured in a preorganized geometry as seen during a geometry optimization without bound ligand in which the loop structure of the ligand-binding pocket linearizes. Instead, through a process of induced fit, arsenate causes the alignment of the catalytic groups in their correct orientation. This is revealed by the observed stabilizing effect on the active site geometry upon ligand binding. Our calculations are in accordance with the kinetic and $^1H-^{15}N$ heteronuclear single quantum correlation nuclear magnetic resonance (HSQC NMR) spectroscopy experiments,[7b] which demonstrated a dynamic character of the active site P-loop in the absence of tetrahedral oxyanions and its stabilization upon binding. Remarkably, three water molecules in the active site appear to be necessary to maintain the loop of the ligand-binding pocket as structured. Without water molecules, the ligand-binding loop linearizes during the geometry optimization. This forms a possible explanation for the observation of four well-defined water molecules in an unliganded active site in the X-ray structure of ArsC wild type (1LJL).[11]

Enzyme−Substrate Interactions. During ligand binding, the desolvation energy has to be overcome and entropy is lost by the stabilization of the ligand-binding loop. To deal with this energetically costly process several favorable enzyme−substrate interactions are formed in the Michaelis complex of which Figure 4 presents an overview. All comparisons were performed with the X-ray structure of pI258 ArsC (PDB: 1LJU),[11] because this structure resembles most the Michaelis complex studied in this work.

To discern which anionic species of arsenate is most likely to be bound in the active site, we compared the interaction energies (calculated at B3LYP/6-31+G**) of mono- and dianionic arsenate with ArsC, calculated as the difference between the energy of the optimized complex and the optimized, isolated arsenate and the noncomplexed enzyme. These two interaction energies contain the same, unknown energy of the noncomplexed enzyme, which cancels upon comparison. The binding of dianionic arsenate turned out to be 82 kcal/mol more favorable than that of monoanionic arsenate, despite the vicinity of the negatively charged Cys10.

In the ArsC−dianionic arsenate complex, all backbone amide hydrogen atoms in the catalytic loop are oriented toward the center of the loop. With the exception of Gly12 and Asn13, they all form hydrogen bonds with the oxygen atoms of dianionic arsenate. All free electron pairs of these oxygens are involved in hydrogen bonding. In the case of a monoanionic arsenate, the extra hydrogen atom on one of the oxygens would experience steric hindrance, making a dianionic form of arsenate more favorable. The nucleophilic S_γCys10 interacts with the Gly12 and Asn13 backbone amide groups and with the hydroxyl group of Ser17 via hydrogen bonds (Figure 4). In the crystal structure of the first reaction step product (PDB: 1LJU),[11] the distances between S_γCys10 and the Gly12 amide, S_γCys10 and the Asn13 amide, S_γCys10 and O_γSer17 are respectively 4.26, 3.65, and 3.28 Å. With the exception of the first interaction, these distances are in the same range as those in the "in silico" obtained Michaelis complex (Figure 4).

Arg16 Guanidinium Group. In the optimized wild-type model, the guanidinium group of Arg16 provides an extension of the substrate-binding pocket, via a spherical structure surrounding the substrate. In LMW PTPase,[2] a crucial Arg is observed at about the same structural position. Nevertheless, the orientation of the ligand in the Michaelis complex of ArsC is quite different from the position taken by the phosphotyrosine substrate in the active site of LMW PTPase. In LMW PTPase, strong hydrogen bonds are formed between $N_\epsilon H/N_\eta H$ of the guanidinium group of the ArsC Arg16 homologue and two nonprotonated oxygen atoms of the substrate.[2] In contrast, in the optimized structure of wild type ArsC, only Arg16N_ηH is involved in a hydrogen bond with a nonprotonated oxygen atom, while Arg16N_ϵH donates a hydrogen bond to the leaving hydroxyl group. This difference in substrate binding between ArsC and LMW PTPase might promote ArsC as an arsenate reductase instead of a PTPase. After a comparison with the X-ray structure of the first reaction step product (1LJU),[11] where Arg16N_ϵ interacts with

TABLE 1: Experimentally Measured K_M and k_{cat} Values for Wild Type and Mutant ArsC[a]

ArsC	K_M (μM)	k_{cat} (min^{-1})	k_{cat}/K_M ($M^{-1}\,s^{-1}$)
wild type	68	215	5.2×10^4
Arg16Lys	no activity		
Asn13Ala	68	29.2	7×10^3
Ser17Ala	79	38	8×10^3

[a] The catalysis of arsenate reductase by pI258 ArsC mutants.[7b,11] Arsenate reductase activity determined in a coupled enzyme assay with Trx, TR, and NADPH under standard assay conditions. No activity means a k_{cat} value lower than 0.08 s^{-1} in an initial velocity experiment in the presence of 20 mM arsenate.

the leaving water molecule (2.96 Å), we can conclude that our calculated model is in full accordance.

True binding energies cannot be obtained since the geometry of the noncomplexed enzyme is not available. Hence, interaction energies are calculated (at B3LYP/6-31+G**) using the extracted geometry of the uncomplexed enzyme from the complexed one. In the Arg16Ala mutant, the interaction with dianionic arsenate is found to be less favorable (123 kcal/mol). This value has to be treated with the necessary caution since structural rearrangements in the enzyme and entropic considerations upon going from the complexed to the uncomplexed form are not taken into account.

With a monoanionic arsenate as ligand, the interaction of the leaving group with Arg16N$_\epsilon$ disappears. As such, the monoanionic substrate−enzyme complex resembles *less the* covalent adduct. As a consequence the binding of a monoanionic substrate is less probable. Further evidence comes from the optimization (MP2/6-31++G**) of the $CH_3S-AsO_3^{2-}$ and the $CH_3-AsHO_3^-$ model systems in the gas phase. The S−As bond distance is respectively 2.32 and 2.23 Å in the optimized dianionic and monoanionic adduct, while the crystallographic (1LJU)[11] value of the S−As bond length is 2.4 Å. This means that the S−As bond length of the optimized dianionic adduct is closest to the one observed in the crystal structure, *further* evidence for dianionic substrate binding.

Asn13Ala Structure. In the in silico optimized Asn13Ala mutant, the enzyme−substrate interactions of the wild-type complex are conserved. The average hydrogen bond length is 2.76 Å and the average donor-H-acceptor angle is 165°, a deviation from the average wild type values by only 0.01 Å and 5° respectively. As such, all interactions of the optimized wild-type ArsC-arsenate complex are maintained in this mutant. This observation is in agreement with the similar K_M values for WT and Asn13Ala ArsC. The low k_{cat} values (Table 1) suggest that K_M is a genuine binding constant.

Reactivity Analysis by Means of the HSAB Principle. The experimentally obtained k_{cat} values for the reduction catalyzed by ArsC are macroscopic rate constants. Apart from the first reaction step considered here, k_{cat} may comprise other microscopic rate constants appearing in the in the successive reaction steps of the catalytic cycle (Figure 1B). As a consequence, no direct information concerning the activation energy of the first reaction step of this multistep reaction mechanism can be deduced from the experimentally obtained kinetic data. Although no microscopic k_{cat} value of the first reaction step is known, the application of the HSAB principle provides information regarding the onset of the first catalyzed step by which more insight in the global k_{cat} is gained.

Application of the HSAB principle offers the advantage that the characteristics of a reaction (mainly kinetic aspects) are described in terms of the properties of the reagents in the ground state, without explicit numerical calculation of characteristics along the reaction path. As such, application of the HSAB principle allows the deduction of relative activation energies from information on the reactant properties only. This principle offers the possibility to interpret and to predict the results of reaction path calculations going along with Parr's dictum "To compute is not to understand."[39]

TABLE 2: Reactivity between As and S in WT and Mutant Enzymatic Environments[a]

model	Δs (au)
WT	1.575
electrophile effect: Arg16Ala	1.601
nucleophile effect: −N13/-K^+	2.269

[a] Reactivity in the enzymatic environment of WT and mutant ArsC as measured by difference in local softness Δs (au) between As and S.

The application of the HSAB principle estimates the interaction strength between two interacting partners by comparing their local softness in the reactant state. This qualitative description of the interaction strength enables us to identify the residues in ArsC responsible for nucleophilic activation in the first reaction step. The reactivity between arsenate and Cys10 increases with decreasing difference in local softness of the two interacting sulfur and arsenic atoms. The difference between the local softness of SγCys10 and arsenic is minimized in the presence of both Arg16 and the C10−K^+ interaction network. Both have a positive impact on the Cys10−arsenate reactivity (Table 2), with the influence of the C10−K^+ interaction network being the most important. According to the HSAB principle, we can argue that the stabilization of the nucleophile is of greater importance than the stabilization of the electrophile, at the onset of the first reaction step, partially explaining the decrease in k_{cat} found for mutant ArsC (Table 1).

Activation of the Electrophile. The active site of ArsC embraces arsenate upon binding, without any significant conformational changes of the arsenate. Compared to free arsenate in gas phase, the mean deviations of the As−O bond lengths and O−As−O angles are respectively 0.026 Å and 3°.

The largest effect of arsenate binding upon its structure is seen for the As- -OH(LG) bond length for which a decrease of 0.096 Å is observed in comparison to free arsenate in gas phase. Since geometrical structures are functions of the electron distribution, this diminished bond length seems natural, because of the observed charge transfer from arsenate to the enzyme (vide infra). In the gas phase, the As−OH bond lengths (fully optimized geometries calculated at B3LYP/6-31+G**) for a diprotonated nonbound arsenate are also shorter than those for monoprotonated nonbound arsenate (0.089 Å).

The As- -OH(LG) bond length in the Arg16Ala mutant shortens with 0.039 Å in comparison to this of the wild type. A significant value, as this is almost four times as much as in the Asn13Ala mutant. A greater bond length signifies a weaker bond and as a consequence a facilitated dissociation of the leaving group. The observation thereof in a Michaelis complex is in line with the catalytic principle of "ground-state destabilization".[40] The elongating of the As- -OH(LG) bond in the wild-type Michaelis complex indicates the importance of Arg16 as ground-state destabilizer.

The energy of the complex with a bound dianionic substrate is 375 kcal/mol higher than the energy of the complex with a bound monoanion. This energy difference correlates with the ground-state destabilization of the bound dianionic arsenate by the arsenate−Arg16N$_\epsilon$ interaction, which is not present in the monoanionic complex.

The sensitivity to nucleophilic attack on a species can be quantified in a DFT context by the electrophilicity index (ω),

TABLE 3: Charge Distribution[a] in Enzyme-Bound and Water-Solved $HAsO_4^{2-}$

	charge distribution (au)	
	WT complex	$HAsO_4^{2-}$ water[b]
As	2.5915	2.4529
O(LG)	−1.1264	−1.1278
O	−1.2656	−1.2705
O	−1.2249	−1.2551
H	0.5427	0.4710
O	−1.2227	−1.2705
charge transfer	0.2945	0

[a] NPA charge distribution (au) in enzyme-bound and water-solvated monoprotonated arsenate ($HAsO_4^{2-}$), calculated at the B3LYP/6-31+G** level. [b] SCI−PCM[33] solvent model used.

TABLE 4: Spillover Effect in the Charge Transfer in the ArsC−Arsenate Hydrogen Bonds

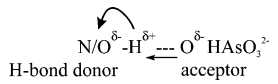

	free enzyme		enzyme−substrate complex	
donor- -acceptor	q(N/O)	q(H)	q(N/O)	q(H)
N_ϵH(Arg16)- -OH(LG)	−0.616	0.449	−0.646	0.484
N_{16}H- -O(1)	−0.670	0.406	−0.683	0.460
N_{17}H- -O(1)	−0.670	0.438	−0.683	0.478
HOH(2)- -O(2)	−1.033	0.473	−1.072	0.537
N_{14}H- -O(2)	−0.670	0.407	−0.668	0.464
N_{11}H- -O(3)	−0.691	0.414	−0.691	0.469
N_ηH(Arg16)- -O(3)	−0.813	0.438	−0.818	0.479
HOH(3)- -O(3)	−1.015	0.482	−1.062	0.534

[a] Spillover effect in the charge in the enzyme−substrate hydrogen bonds in the ArsC Michaelis complex. The arrows indicate the direction of negative charge flow. NPA charges (Q) are calculated (B3LYP/6-31+G**) on the enzyme−substrate complex (WT model) and on the nonbounded catalytic loop of ArsC. Coordinates of the free catalytic site are taken from the optimized geometry of the WT Michaelis complex.

calculated with eq 10. Herein, the ionization energy (I) and the electron affinity (A) are set equal to zero when negative values are found. If I and A are both negative, ω is beyond its action radius and loses its meaning, which is the case for free arsenate in gas phase. In the wild-type complex, bound arsenate has an ω value equal to 5 kcal/mol, whereas ω for arsenate in the Arg16Ala mutant is again meaningless, indicating that Arg16 has a positive influence on the electrophilicity of arsenate and as a consequence on the accessibility of arsenate to the nucleophilic attack.

The critical function of Arg16 in As- -OH(LG) bond length extension and on the electrophilicity of arsenate makes this residue highly important in the reactant state. As such it was not at all a surprise to observe a *dramatic* drop in activity of the Arg16Lys mutant (Table 1), the moment the NϵH was removed.

One of the most important and intuitive arguments against a dianionic substrate in the enzymatic mechanism is the Coulomb repulsion with the proximal nucleophilic thiolate.[4] Nevertheless, the nucleophilic attack on a dianionic substrate has been proposed[5] on the basis of predicted reactivities and calculated interaction energies between sulfur and arsenic: obtained through the application of the HSAB[6] principle. We observed that the difference in softness between arsenic and sulfur decreases as arsenate becomes more deprotonated (softer). This was observed in the gas phase as well as in an enzymatic environment, modeled with a dielectric constant of 20.7.[41] In the present study, the total calculated charge on arsenate in the wild-type Michaelis complex (−1.71 unit charges) clearly demonstrates a charge transfer to the enzyme (Table 3). This means that through the numerous enzyme−substrate interactions in the reactant state the original dianionic substrate passes into a decreased dianionic state by binding. This negative charge stabilization reduces the electrostatic repulsion in the enzyme and hence partially explains the binding of a dianionic substrate.

Consider the enzyme−substrate interactions $N/O^{\delta-}-H^{\delta+}$- - - $O^{\delta-}HAsO_3^{2-}$, with N/O−H the backbone amide or water hydrogen bond donors and $OHAsO_3^{2-}$ (arsenate) the hydrogen bond acceptor. A brief analysis of the charge transfer (Table 4) indicates that the spillover effect of the negative charge, as described for donor−acceptor interactions in general by Gutman,[42] is also found in the ArsC−arsenate hydrogen bonds, apart from two exceptions: the N_{14}H- -O(2) and the N_{11}H- -O(3) interactions (Table 4). Upon arsenate binding, the negative charge is transferred from arsenate to ArsC. As the hydrogen atoms of the backbone amides and the water molecules directly interact with the substrate arsenate, they are the first acceptors of the transmitted negative charge. However, the fractional positive charge (δ^+) on the hydrogen atoms of the hydrogen bond donors increases. The negative charge from arsenate is transmitted via these hydrogen atoms to the nitrogen and oxygen atoms of the hydrogen bond donors. In this way the fractional negative charges of the nitrogen and oxygen atoms increase. (Table 4) In small molecules, it is well-known[42] that, after this first spillover transmission, the negative charge is transferred further to the terminal atoms. In the enzyme, terminal atoms are at very large distances, so that the transferred charge is delocalized over the system.

The charge transfer from arsenate to ArsC is accompanied by a charge rearrangement within arsenate in such a way that the central arsenic atom becomes more positive compared to unbound arsenate (0.149 unit charges, almost half of the observed charge transfer of 0.294 unit charges), while the charges on the oxygen atoms remain more or less the same. Along with this increase in positive charge, the central arsenic atom becomes more electrophilic as quantitatively measured by the local electrophilicity ω^+ (eq 11). ω^+ passes from meaningless (vide supra) for the arsenic atom of free arsenate in gas phase toward 4 kcal/mol upon binding. As a consequence, arsenic becomes more receptive to the nucleophilic attack, and is activated by binding to ArsC.

Activation of the Nucleophile. At the optimum pH for enzymatic catalysis by ArsC (pH = 8.0),[7b] a substantial amount of free cysteine (pK_a = 8.3) is present in the thiolate form. In the enzyme−substrate complex, however, the presence of dianionic arsenate in the vicinity of Cys10 is expected to increase the latter's basicity and to drive the thiol/thiolate equilibrium toward the thiol form, which is a weaker nucleophile compared to the thiolate form.[8] However, it can be anticipated that the enzymatic environment favors the deprotonated state.

Apart from the backbone amide hydrogens of Gly 12 and Asn 13, Ser 17 is the only residue that interacts directly with Cys10.[11] Since Ser17 cannot function as a general base, general base catalysis can be excluded. Rather, we strongly suggest nucleophilic catalysis with a stabilized thiolate form in the reactant state. Hydrogen bonds are known to have a pK_a lowering effect on the acceptor molecule, especially when the donor molecule is positively charged.[43] However, this is not the case for the Cys10Sγ- -H−OγSer17 hydrogen bond in pI258 ArsC and as such it is unlikely that this single interaction will

sufficiently suppress the pK_a of Cys10. As a consequence, one can think of a possible role for the C10−K^+ interaction network (Figure 2) in strengthening the Cys10Sγ- -H−OγSer17 hydrogen bond.

Under the influence of Asn13 and potassium, a clear displacement of the hydrogen from H−OγSer17 toward SγCys10 is observed (Figure 2). Asn13 and potassium have the same impact on the Cys10Sγ- -H−OγSer17 distance and their effect is additive (Figure 2). The shortening of the Cys10Sγ- -H−OγSer17 distance, when inserting the elements of the network one by one, is in agreement with the increase of the SγCys10−H−OγSer17 hydrogen bond strength. Also here, an additive effect of Asn13 and potassium is observed (Figure 2). Under the impulse of potassium, the Asn13-Nϵ-hydrogen moves toward OγSer17 (Figure 2).

As mentioned before in the Introduction, the experimental determination of the pK_a is not straightforward because three of the four cysteine residues present in pI258 ArsC are involved in the reaction mechanism (Figure 1B). However, evidence for a shifted pK_a can be given from high level theoretical calculations.[14d] Figure 5 gives a proton affinity−pK_a calibration curve ($R^2 = 0.88$) for a series of substituted thiolates. Herein, the calculated proton affinities of methanethiol (as model system for Cys10) in the presence of different elements of the C10−K^+ network are implemented. In the presence of the single SγCys10- -H−OγSer17 hydrogen bond, a decrease of the pK_a with 0.3 units is observed. When Asn13 and K^+ are completing the C10−K^+ network, an additional decrease of the pK_a with respectively 3.4 and 0.4 units is found, yielding a final pK_a of methanethiol in the presence of the hydrogen bond network of 6.2. As such, Cys10 can be predicted to be mainly deprotonated in the range of maximal catalytic activity of ArsC. The relative importance of Ser17 and Asn13 on the pK_a of Cys10 correlates with a drop of the experimentally measured k_{cat} values (Table 1) with factors of about 7 and 5 for the Asn13 and the Ser17 mutation, respectively. Previously, the increase of k_{cat}/K_M[10] in the presence of K^+ has been explained by its role in the thermal stabilization of ArsC.[10] Here, we showed the importance of K^+ for the activation of the nucleophilic Cys10.

ArsC is suggested to be evolved from an ancestral LMW PTPase,[1] but there, no K^+ is present at this binding site. In bovine and human LMW PTPases,[44] the imidazole side chain of His72 occupies the space of the potassium binding site.[10] More specifically, the potassium coincides precisely with the (protonated) Nϵ2 of His72, which makes contacts within hydrogen bonding distance with the structurally and sequentially conserved Asn and Ser.[1,10] Potassium ions are particularly suited for replacing protonated histidine residues, while maintaining similar interactions with the neighbor residues. Both have a single positive charge and the ionic radius of potassium allows it to coordinate to oxygens with bond distances similar to those of hydrogen bonds. In LMW PTPases, the His-K^+ substitution is not only structurally conservative, but also functionally. The histidine imidazole has been shown to contribute significantly to enzyme stability[45] as well as to stabilize the thiolate anion of the nucleophilic cysteine by lowering its pK_a,[45] exactly the two functions observed for K^+ in ArsC.

In the crystal structure of the oxidized ArsC C89L mutant,[11] the Cys10-Cys82 disulfide bridge is formed and a negatively charged chloride ion occupies the position of the Cys10 thiolate in the reduced form, indicating the importance of maintaining the C10−K^+ interaction network—starting from a negative charge. On the basis of the importance of the C10−K^+ interaction network in the stabilization of the Cys10 thiolate, the drop of the experimentally measured k_{cat} values (Table 1) for mutant ArsC can be explained.

An extra decrease of the pK_a with 0.2 units is calculated for the macrodipole moment exerted by the α-helix spanning residues 16 to 29, which brings the final Cys10 pK_a in *S. aureus* pI258 ArsC to 6.0 (Figure 5). As mentioned before, the experimental determination of the Cys10 pK_a value in pI258 ArsC is not evident. For *Escherichia coli* R773 ArsC,[7a] however, the experimental pK_a value of the Cys10 *S. aureus* pI258 ArsC analogue is 6.3 in the presence of a charged histidine residue.[7a] Although the pK_a values of the nucleophilic cysteines of both *S. aureus* and *E. coli* ArsC are of similar magnitude, the two ArsC families are not related. As a consequence, we can conclude that an analogous evolution has taken place. The *S. aureus* pI258 ArsC C10−K^+ interaction network and the *E. coli* R773 ArsC histidine residue have developed separately to deal with the same problem of activation of the nucleophile.

Conclusion

Starting from the X-ray structure of the first reaction step product, the two-layer QM/QM ONIOM method provides a reliable structure of the Michaelis complex of ArsC. Arsenate binding stabilizes the loop structure of the active site.

Activation of the electrophile in the Michaelis complex of pI258 ArsC takes place by a charge transfer from arsenate to the enzyme during the formation of the enzyme−substrate complex. In particular, the central arsenic atom becomes more positively charged rendering the substrate more electrophilic and more susceptible to nucleophilic attack. The observed charge transfer strengthens the evidence for a dianionic arsenate in the presence of a negatively charged sulfur on the nucleophilic Cys10. Moreover, the interaction with the N_ϵ of Arg16 increases the bond length of the As−OH(LG) bond and will finally lead to the breaking of this bond in the reaction state.

Stabilization of the nucleophilic thiolate form of Cys10 is accomplished by decreasing its pK_a to 6.0 by both the macrodipole of a nearby α-helix and the interaction network from SγCys10 via HOγSer17 and HN$_\delta$Asn13 to potassium.

All together, the use of DFT and the application of the HSAB principle leads to conclusions that were unpredictable only based on X-ray structures and steady-state kinetic data. This gives the theoretical model approach an extra dimension in the explanation of experimental data.

Acknowledgment. P.G. and L.W. thank the Fund for Scientific Research Flanders (FWO) and the VUB for continuous support of their research groups. S.L. thanks the Fund for Scientific Research Flanders (FWO) for a postdoctoral fellowship. G.R. thanks the Fund for Scientific Research Flanders (FWO) for a predoctoral fellowship (Aspirant). The crystal structures discussed in this work were obtained using data collected at the European Molecular Biology Laboratory (EMBL) Hamburg Outstation and at the European Synchrotron Radiation Facility, Grenoble, France.

Supporting Information Available: A table of Cartesian coordinates (Å) of the optimized (two-layer ONIOM scheme: B3LYP/6-31+G**//HF/6-31G) Michaelis complex (WT) and the Asn13Ala and the Arg16Ala mutants and text and tables giving a detailed explanation about obtaining the values of the difference in interaction energies of (1) mono- and dianionic arsenate in WT ArsC and (2) dianionic arsenate in WT and Arg16Ala ArsC. This material is available free of charge via the Internet at http://pubs.acs.org.

References and Notes

(1) Zegers, I.; Martins, J. C.; Willem, R.; Wyns, L.; Messens, J. *Nature: Struct. Biol.* **2001**, *8*, 843.

(2) Zhang, Z.-Y. *Crit. Rev. Biochem. Mol. Biol.* **1998**, *33*, 1.

(3) (a) Czyryca, P. G.; Hengge, A. C. *Biochim. Biophys. Acta* **2001**, *1547*, 245. (b) Asthagiri, D.; Dillet, V.; Liu, T.; Noodleman, L.; Van Etten, R.; Bashford, D. *J. Am. Chem. Soc.* **2002**, *124*, 10225.

(4) (a) Hansson, T.; Nordlund, P.; Åqvist, J. *J. Mol. Biol.* **1997**, *265*, 118. (b) Kolmodin, K.; Nordlund, P.; Åqvist, J. *Proteins: Struct., Funct. Genet.* **1999**, *36*, 370. (c) Kolmodin, K.; Åqvist, J. *FEBS Lett.* **2001**, *498*, 208.

(5) Roos, G.; Loverix, S.; De Proft, F.; Wyns, L.; Geerlings, P. *J. Phys. Chem. A* **2003**, *107*, 6828.

(6) Pearson, R. G. *Chemical Hardness*; Wiley-VCH: Weinheim, Germany, 1997.

(7) (a) Gladysheva, T.; Liu, J.; Rosen, B. P. *J. Biol. Chem.* **1996**, *271*, 33256. (b) Messens, J.; Martins, J. C.; Brosens, E.; Van Belle, K.; Jacobs, D. M.; Willem, R.; Wyns, L. *J. Biol. Inorg. Chem.* **2002**, *7*, 146.

(8) Dantzman, C. L.; Kiessling, L. L. *J. Am. Chem. Soc.* **1997**, *118*, 111715.

(9) Fersht, A. *Enzyme Structure and Mechanism*; W. H. Freeman and Co.: New York, 1984.

(10) Lah, N.; Lah, J.; Zegers, I.; Wyns, L.; Messens, J. *J. Biol. Chem.* **2003**, *278*, 24673.

(11) Messens, J.; Martins, J. C.; Van Belle, K.; Brosens, E.; Desmyter, A.; De Gieter, M.; Wieruszeski, J.-M.; Willem, R.; Wyns, L.; Zegers, I. *Proc. Natl. Acad. Sci. U.S.A.* **2002**, *99*, 8506.

(12) (a) Parr, R. G.; Yang, W. *Density-Functional Theory of Atoms and Molecules*, Oxford University Press: Oxford, Englamd, 1989. (b) Koch, C. W.; Holthausen, M. C. *A Chemist's Guide to Density Functional Theory*, 2nd ed.; Wiley VCH: Weinheim, Germany, 2001.

(13) (a) Parr, R. G.; Yang, W. *Annu. Rev. Phys. Chem.* **1995**, *46*, 701. (b) Geerlings, P.; De Proft, F.; Langenaeker, W. *Adv. Quantum Chem.* **1999**, *33*, 303. (c) Chermette, H. *J. Comput. Chem.* **1999**, *20*, 129. (d) Geerlings, P.; De Proft, F. *Int. J. Quantum Chem.* **2000**, *80*, 227. (e) De Proft, F.; Geerlings, P. *Chem. Rev.* **2001**, *101*, 1451. (f) Geerlings, P.; De Proft, F.; Langenaeker, W. *Chem. Rev.* **2003**, *103*, 1793.

(14) (a) Baeten, A.; Maes, D.; Geerlings, P. *J. Theor. Biol.* **1998**, *195*, 2711. (b) Mignon, P.; Steyaert, J.; Loris, R.; Geerlings, P.; Loverix, S. *J. Biol. Chem.* **2002**, *277*, 36770. (c) Mignon, P.; Loverix, S.; Steyaert, J.; Geerlings, P. *Int. J. Quantum Chem.* **2004**, *99*, 53. (d) Versees, W.; Loverix, S.; Vandemeulebroeke, A.; P. Geerlings, Steyaert, J. *J. Mol. Biol.* **2004**, *338*, 1.

(15) (a) Yang, W.; Parr, R. G. *Proc. Natl. Acad. Sci. U.S.A.* **1985**, *82*, 6723. (b) Parr, R. G.; Yang, W. *J. Am. Chem. Soc.* **1984**, *106*, 4049.

(16) Koopmans, T. A. *Physica* **1933**, *1*, 104.

(17) (a) Parr, R. G.; Szentpaly, L. V.; Liu, S. *J. Am. Chem. Soc.* **1999**, *121*, 1922. (b) Maynard, A. T.; Huang, M.; Rice, W. G.; Covell, D. G. *Proc. Natl. Acad. Sci. U.S.A.* **1998**, *95*, 11578. (c) Domingo, L. R.; Aurell, M. J.; Perez, P.; Contreras, R. *J. Phys. Chem. A* **2002**, *106*, 6871.

(18) (a) Perez, P.; Andres, J.; Safont, V. S.; Tapia, O.; Contreras, R. *J. Phys. Chem. A* **2002**, *106*, 5353. (b) Olah, J.; De Proft, F.; Veszpremi, T.; Geerlings, P. *J. Phys. Chem. A* **2004**, *108*, 490.

(19) (a) SPARTAN version 5.0, Wavefunction, Inc., 18401 Von Karman Av., Ste. 370, Irvine, CA 92612. (b) Halgren, T. A. *J. Comput. Chem.* **1996**, *17*, 490.

(20) Svensson, M.; Humbel, S.; Froese, R. D. J.; Sieber, S.; Morokuma, K. *J. Phys. Chem.* **1996**, *100*, 19357.

(21) Dapprich, S.; Komáromi, I.; Byun, K. S.; Morokuma, K.; Frisch, M. J. *J. Mol. Struct. (THEOCHEM)* **1999**, *462*, 1.

(22) (a) Torrent, M.; Vreven, T.; Musaev, G.; Morokuma, K.; Farkas, O.; Schlegel, H. B. *J. Am. Chem. Soc.* **2002**, *124*, 192. (b) Vreven, T.; Morokuma, K. *J. Phys. Chem. A* **2002**, *106*, 6167.

(23) Vreven, T.; Morokuma, K.; Farkas, Ö.; Schlegel, B. J.; Frisch, M. J. *J. Comput. Chem.* **2003**, *24*, 760.

(24) Reed, A. E.; Curtiss, L. A.; Weinhold, F. *Chem. Rev.* **1988**, *88*, 899.

(25) Bachrach, S. M. In *Reviews in Computational Chemistry*; Lipkowitz, K. B., Boyd, D. B., Eds.; VCH: New York, 1997; Vol. V.

(26) Jensen, F. *Introduction to Computational Chemistry*; John Wiley and Sons: New York, 1999.

(27) (a) Breneman, C. M.; Wiberg, K. B. *J. Comput. Chem.* **1990**, *11*, 361. (b) Hayes, D. M.; Kollman, P. A. *J. Am. Chem. Soc.* **1976**, *98*, 3335.

(28) (a) Bultinck, P.; Langenaeker, W.; Lahorte, W.; De Proft, F.; Geerlings, P.; Waroquier, M.; Tollenaere, J. P. *J. Phys. Chem. A* **2002**, *106*, 7887. (b) Bultinck, P.; Langenaeker, W.; Lahorte, W.; De Proft, F.; Geerlings, P.; Van Alsenoy, C.; Tollenaere, J. P. *J. Phys. Chem. A* **2002**, *106*, 7895.

(29) (a) Boys, S. F.; Bernardi, F. *Mol. Phys.* **1970**, *19*, 553. (b) Van Duijneveldt, F. B.; Van Duijneveldt-Van de Rijdt, J. G. C. M.; Van Lenthe, J. H. *Chem. Rev.* **1994**, *94*, 1873.

(30) (a) Smallwood, J. C.; McAllister, M. A. *J. Am. Chem. Soc.* **1997**, *119*, 11277. (b) Pan, Y.; McAllister, M. A. *J. Am. Chem. Soc.* **1997**, *119*, 7561.

(31) Sigfridsson, E.; Ryde, U. *J. Comput. Chem.* **1998**, *19*, 377.

(32) Peräkylä, M. *Phys. Chem. Chem. Phys.* **1999**, *24*, 5643.

(33) (a) Tomasi, J.; Perisco, M. *Chem. Rev.* **1994**, *94*, 2027. (b) Wiberg, K. B.; Keith, T. A.; Frisch, M. J.; Murcko, M. *J. Phys. Chem.* **1995**, *99*, 9072. (c) Foresman, J. B.; Frisch, A. E. *Exploring Chemistry with Electronic Structure Methods*, 2nd ed.; Gaussian, Inc.: Pittsburgh, PA, 1996. (d) Safi, B.; Choho, K.; De Proft, F.; Geerlings, P. *J. Phys. Chem. A* **1998**, *102*, 5253. (e) Safi, B.; Choho, K.; Geerlings, P. *J. Phys. Chem. A.* **2001**, *105*, 591.

(34) Frisch, M. J.; Trucks, G. W.; Schlegel, H. B.; Scuseria, G. E.; Robb, M. A.; Cheeseman, J. R.; Montgomery, J. A., Jr.; Vreven, T.; Kudin, K. N.; Burant, J. C.; Millam, J. M.; Iyengar, S. S.; Tomasi, J.; Barone, V.; Mennucci, B.; Cossi, M.; Scalmani, G.; Rega, N.; Petersson, G. A.; Nakatsuji, H.; Hada, M.; Ehara, M.; Toyota, K.; Fukuda, R.; Hasegawa, J.; Ishida, M.; Nakajima, T.; Honda, Y.; Kitao, O.; Nakai, H.; Klene, M.; Li, X.; Knox, J. E.; Hratchian, H. P.; Cross, J. B.; Adamo, C.; Jaramillo, J.; Gomperts, R.; Stratmann, R. E.; Yazyev, O.; Austin, A. J.; Cammi, R.; Pomelli, C.; Ochterski, J. W.; Ayala, P. Y.; Morokuma, K.; Voth, G. A.; Salvador, P.; Dannenberg, J. J.; Zakrzewski, V. G.; Dapprich, S.; Daniels, A. D.; Strain, M. C.; Farkas, O.; Malick, D. K.; Rabuck, A. D.; Raghavachari, K.; Foresman, J. B.; Ortiz, J. V.; Cui, Q.; Baboul, A. G.; Clifford, S.; Cioslowski, J.; Stefanov, B. B.; Liu, G.; Liashenko, A.; Piskorz, P.; Komaromi, I.; Martin, R. L.; Fox, D. J.; Keith, T.; Al-Laham, M. A.; Peng, C. Y.; Nanayakkara, A.; Challacombe, M.; Gill, P. M. W.; Johnson, B.; Chen, W.; Wong, M. W.; Gonzalez, C.; Pople, J. A. *Gaussian 03*, revision A.01. Gaussian, Inc.: Pittsburgh, PA, 2003.

(35) Fauman, E. B.; Yuvaniyama, C.; Schubert, H. L.; St, Saper, M. A. *J. Biol. Chem.* **1996**, *271*, 18780.

(36) Schubert, H. L.; Fauman, E. B.; Stuckey, J. A.; Dixon, J. E.; Saper, M. A. *Protein Sci.* **1995**, *4*, 1904.

(37) (a) Scarsdale, J. N.; Van Alsenoy, C.; Klimkowski, V. J.; Schaefer, L.; Momany, F. A. *J. Am. Chem. Soc.* **1983**, *105*, 3438. (b) Ramachandran, G. N. *Biopolymers* **1968**, *6*, 1494.

(38) (a) Rajagopalan, P. T.; Benkovic, S. J. *Chem. Rec.* **2002**, *2*, 24. (b) Benkovic, S. J.; Hammes-Schiffer, S. *Science* **2003**, *301*, 5637. (c) Warshel, A. *J. Biol. Chem.* **1998**, *273*, 27035. (d) Bruice, T. C.; Benkovic, S. J. *Biochemistry* **2000**, *39*, 6268. (e) Rishavy, M. A.; Cleland, W. W.; *Biochemistry* **2000**, *39*, 4569. (f) Bruice, T. *Acc. Chem. Res.* **2002**, *35*, 139. (g) Warshel, A.; Florián, J.; Štrajbl, M.; Villà, J. *Chembiochem.* **2001**, *2*, 109. (h). Shurki, A.; Štrajbl, M.; Villà, J.; Warshel, A. *J. Am. Chem. Soc.* **2002**, *124*, 4097.

(39) Parr, R. G. Density Functional Theory in Chemistry. In *Density Functional Methods in Physics*; Dreizler, R. M., da Providencia, J., Eds.; Plenum: New York, 1985; p 141.

(40) (a) Bayliss, W. M., Sir. *The Nature of Enzyme Action*, 5th ed.; Longmans, Green & Co.: London, 1925. (b) Haldane, J. B. S. *Enzymes*; Longmans, Green & Co.: London, 1930.

(41) (a) Fitch, C. A.; Karp, D. A.; Lee, K. K.; Stites, W. E.; Lattman, E. E.; Garcia-Moreno, E. B. *Biophys. J.* **2002**, *82*, 3289. (b) Schutz, C.; Warshel, A. *Proteins: Struct., Funct. Genet.* **2001**, *44*, 400. (c) Dillet, V.; Van Etten, R.; Bashford, D. *J. Phys. Chem. B* **2000**, *104*, 11321.

(42) (a) Gutman, V. *The Donor−Acceptor Approach to Molecular Interactions*; Plenum Press: New York and London, 1978. (b) Geerlings, P.; Tariel, N.; Botrel, A.; Lissillour, R.; Mortier, W. J. *J. Phys. Chem.* **1984**, *88*, 5752.

(43) Jeffrey, G. A. *An Introduction to Hydrogen Bonding*; Oxford University Press: New York, 1997.

(44) (a) Logan, T. M.; Zhou, M. M.; Nettesheim, D. G.; Meadows, R. P. Van Etten, R. L.; Fesik, S. W. *Biochemistry* **1994**, *33*, 11087. (b) Zhang, M.; Van Etten, R. L.; Staufacher, C. V. *Biochemistry* **1994**, *33*, 11097. (c) Zhang, M.; Stauffacher, C. V.; Lin, D.; Van Etten, R. L. *J. Biol. Chem.* **1998**, *273*, 21714.

(45) Thomas, C. L.; McKinnon, E.; Granger, B. L.; Harms, E.; Van Etten, R. L. *Biochemistry* **2002**, *41*, 15601.